Applied Catalysis B: Environmental 96 (2010) 307–313

Contents lists available at ScienceDirect

Applied Catalysis B: Environmental

journal homepage: www.elsevier.com/locate/apcatb

# Aqueous bromate reduction by catalytic hydrogenation over $Pd/Al_2O_3$ catalysts

Huan Chen[a], Zhaoyi Xu[a], Haiqin Wan[a], Jianzhong Zheng[a], Daqiang Yin[b,*], Shourong Zheng[a,**]

[a] State Key Laboratory of Pollution Control and Resource Reuse, School of the Environment, Nanjing University, Nanjing 210093, China
[b] Key Laboratory of Yangtze River Water Environment of Ministry of Education, Tongji University, Shanghai 200092, China

ARTICLE INFO

*Article history:*
Received 2 November 2009
Received in revised form 12 February 2010
Accepted 12 February 2010
Available online 21 February 2010

*Keywords:*
Bromate reduction
Catalytic hydrogenation
$Pd/Al_2O_3$ catalyst

ABSTRACT

Bromate is recognized as an oxyhalide disinfection byproduct in drinking water. In this study, supported noble metal (Pd, Pt) catalysts with different supports of $SiO_2$, $Al_2O_3$ and activated carbon (AC) were prepared and the catalytic hydrogenation of aqueous bromate was first investigated. Characterization results showed the isoelectric points (IEPs) of $Pd/SiO_2$ and $Pd/Al_2O_3$ catalysts were around 2.0 and 8.0, respectively, whereas the IEP of Pd/AC was much lower than 2.0. In comparison with $Pd/SiO_2$ and Pd/AC, $Pd/Al_2O_3$ exhibited a substantially higher catalytic activity at pH 5.6 for bromate reduction due to the electrostatic attractive interaction between the bromate ion and the catalyst. Moreover, bromate with an initial concentration of 0.39 mM was removed by 80.2% over $Pt/Al_2O_3$ and nearly 100% over $Pd/Al_2O_3$ after reaction for 2 h, indicative of a higher catalytic activity of $Pd/Al_2O_3$. For $Pd/Al_2O_3$, the bromate reduction followed the Langmuir–Hinshelwood model, reflecting an adsorption controlled reduction mechanism. Increasing Pd loading amount resulted in enhanced bromate reduction. In addition, the bromate reduction was found to be strongly pH-dependent and enhanced reduction rate could be achieved at low pH. In the presence of coexisting anions ($Cl^-$, $Br^-$ and $SO_4^{2-}$) the bromate reduction was suppressed, wherein $SO_4^{2-}$ exhibited the most marked inhibition effect, attributed to competitive adsorption for active surface sites. The present results indicate that catalytic hydrogenation can be used as a potential treatment technique for the removal of bromate in drinking water.



## 1. Introduction

Bromate is an oxyhalide disinfection byproduct frequently detected in drinking water from ozonation or chlorination of bromide-containing source waters [1,2]. Because bromate is a potential carcinogen to humans, the World Health Organization (WHO) and the United States Environmental Protection Agency (USEPA) have strictly regulated the bromate level in drinking water [2,3]. Thus, it is highly desirable to develop effective treatment methods to remove bromate from drinking water.

A variety of treatment techniques have been explored to eliminate bromate pollution in drinking water. Biological technique is effective to reduce bromate to bromide using glucose, pyruvate, formate or starch as electron donors [4,5]. However, the continuous release of biomass and excessive organic compounds during the treatment process limits the practical use of the technique [6]. Alternatively, chemical reduction provides more efficient and cost effective approaches to reduce bromate. For example, bromate reduction by zero-valent iron has been intensively studied [7,8]. However, additional treatment processes are generally necessary for the removal of $Fe^{2+}$ formed in the reaction process due to the stringent regulation on $Fe^{2+}$ concentration in drinking water [9]. Other chemical reduction approaches, such as activated carbon adsorption/reduction and photocatalysis, have also been explored for the removal of aqueous bromate [10–12]. More recently, Kishimoto and Matsuda [13] reported a novel electrochemical method to reduce bromate to bromide under mild reaction conditions.

Catalytic hydrogenation has been recognized as an effective treatment technique to remove undesirable chemical substances in water. Vorlop and Tacke [14] first developed the catalytic hydrogenation method using supported bimetallic catalysts to selectively and effectively reduce aqueous nitrate into $N_2$ [15,16]. In parallel, Hurley and Shapley [17] studied the catalytic hydrogenation of perchlorate in water and observed high catalytic activity of Re–Pd/C under mild reaction conditions. Furthermore, catalytic hydrogenation has also been found to be effective in dechlorination of chlorinated organic contaminants in water [18–22]. Hoke et al. [18] demonstrated that chlorophenols could be feasibly reduced to phenols by catalytic hydrodechlorination over Pd/C catalyst. Gomez-Quero et al. [22] studied the aqueous-phase catalytic hydrogenation of 2,4-dichlorophenol over $Pd/Al_2O_3$ and pointed out that the hydrodechlorination was associated with the surface dispersion of Pd. Considering the oxidative nature of bromate, it is reasonable to hypothesize that the catalytic hydrogenation is also

* Corresponding author. Tel.: +86 21 65982688; fax: +86 21 65982688.
** Corresponding author. Tel.: +86 25 83595831; fax: +86 25 83707304.
*E-mail addresses:* yindq@mail.tongji.edu.cn (D. Yin), srzheng@nju.edu.cn (S. Zheng).

0926-3373/$ – see front matter © 2010 Elsevier B.V. All rights reserved.
doi:10.1016/j.apcatb.2010.02.021

effective for reductive removal of aqueous bromate. To the best of our knowledge, relevant studies have not yet been reported thus far.

The objective of this study was to explore the feasibility of bromate reduction by catalytic hydrogenation over supported noble metal catalysts. A series of catalysts with different noble metals and supports were prepared and further characterized by X-ray diffraction (XRD), transmission electron microscopy (TEM), $N_2$ adsorption, $H_2$ chemisorption, temperature programmed reduction (TPR) and zeta potential ($\zeta$) measurements. The influence of reaction conditions on the bromate reduction was systematically investigated. The results showed that $Pd/Al_2O_3$ exhibited promising catalytic activity toward the bromate reduction, highlighting the potential of catalytic hydrogenation as an effective approach to eliminate bromate contamination in drinking water.

## 2. Experimental

### 2.1. Materials

Commercial activated carbon (Huajing Co., China) was a coconut shell based powdered activated carbon with BET surface area of 624 $m^2\,g^{-1}$. $Al_2O_3$ with BET surface area of 122.4 $m^2\,g^{-1}$ and $SiO_2$ with BET surface area of 132 $m^2\,g^{-1}$ were obtained from Shanghai Chem. Co., China.

### 2.2. Catalyst preparation

The catalysts were prepared by the conventional impregnation method. Briefly, $Al_2O_3$, $SiO_2$ or AC was impregnated by $Pd(Cl)_2$ or $H_2Pt(Cl)_6$ solution under stirring, followed by drying at 120 °C for 2 h, calcining at 300 °C for 2 h in air and subsequently reducing at 300 °C under $H_2$ atmosphere for 4 h. The resulting supported Pd catalyst is denoted as $Pd(x)/Al_2O_3$, where $x$ is the Pd loading amount (wt.%).

### 2.3. Catalyst characterization

XRD patterns of the catalysts were recorded on a Rigaku D/max-RA powder diffraction-meter. Pd contents in the catalysts were determined using inductive coupled plasma emission spectrometer (ICP). TEM images of the samples were obtained on a JEM-2100 transmission electron microscope. BET specific surface areas of the samples were measured using the $N_2$ adsorption method on a Micromeritics ASAP 2200 instrument. Prior to the measurement the samples were pre-treated at 300 °C under vacuum (1.33 Pa) for 1 h.

Pd dispersion of the catalyst was measured using the $H_2$ chemisorption method. Typically, 100 mg of the reduced catalyst was loaded in a U-shaped quartz tube, in which the catalyst was activated in a $H_2$ flow (40 mL $min^{-1}$) at 300 °C for 1 h. After purging with an Ar flow (30 mL $min^{-1}$) for 1 h, the catalyst was cooled down to room temperature. The $H_2$ chemisorption was performed using the pulse titration model with $H_2$ partial pressure below 0.011 atm in each pulse to avoid the formation of β-PdH [23]. $H_2$ contents in the pulses were monitored by a thermal conductivity detector (TCD).

Prior to the reduction of supported catalysts, TPR of the calcined samples was conducted on a home-made apparatus consisting of a gas chromatogram (GC) equipped with a TCD detector. Briefly, 100 mg of the sample was pressed into wafers, broken into small platelets and charged into a U-shaped quartz tube. The sample was preheated at 300 °C in a He flow (30 mL $min^{-1}$) for 2 h. After cooling to room temperature, the sample was heated to 500 °C under a flow gas consisting of 10% $H_2$ in Ar (30 mL $min^{-1}$) at a ramping rate of 10 °C $min^{-1}$. The $H_2$ consumption amount was monitored by an on-line GC and the $H_2$ consumption peaks were normalized on the basis of sample mass.

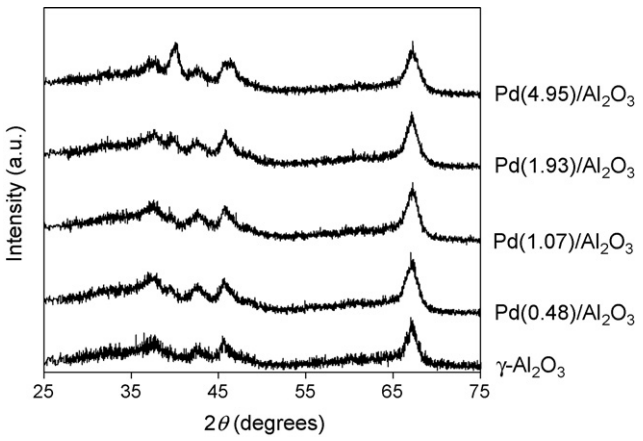


**Fig. 1.** XRD patterns of $Pd/Al_2O_3$ catalysts.

Surface zeta potentials of the samples were measured using a Zeta Potential Analyzer (Zeta PALS, Brookhaven Instruments Co.). Typically, 10 mg of the samples were dispersed in 100 mL of deionized water and the suspension pH was adjusted with either 0.1 M HCl or 0.1 M NaOH equilibrated for 24 h prior to measurement.

### 2.4. Catalytic bromate reduction

Catalytic reduction experiments were carried out at room temperature and atmospheric pressure in a four-necked flask batch reactor equipped with a pH-stat, $H_2$ inlet and outlet, and a sampling port. Briefly, 10 mg of the catalyst was added into the reactor containing 190 mL of distilled water followed by purging the reaction system with a $H_2$ flow (40 mL $min^{-1}$) for 1 h under stirring. Then, 10 mL of 8.0 mM bromate solution was added rapidly into the suspension system which was continuously bubbled by a $H_2$ flow (40 mL $min^{-1}$) under stirring. Samples were taken at selected time intervals and the catalyst particles were removed using 0.45 μm filter. The concentration of bromate in the filtrate was analyzed using Ion Chromatography (ICS1000, Dionex). The initial activity of the catalyst was evaluated using the specific removal rate of bromate within initial 10 min.

## 3. Results and discussion

### 3.1. Catalyst characterization

XRD patterns of $Pd/Al_2O_3$ catalysts with varied Pd loading amounts are shown in Fig. 1. Diffraction peaks characteristic of γ-$Al_2O_3$ were observed at 37.2°, 42.6°, 45.7° and 67.2°. For $Pd/Al_2O_3$ catalysts, new diffraction peaks presented at 40.2° and 46.8°, assigned to typical Pd metal with face centered cubic (fcc) crystallographic structure [24]. In addition, increasing Pd loading amount led to increased intensities of diffraction peaks associated with Pd metal particles, reflecting a higher content of Pd particles and/or larger Pd particles on the $Al_2O_3$ surface with the increase of Pd loading amount (Table 1).

Surface zeta potentials ($\zeta$) of the catalysts as a function of pH are presented in Fig. 2. For all catalysts, zeta potentials continuously decreased with pH. For $Pd/SiO_2$, the isoelectric point (IEP) was around 2.0, nearly identical to that of amorphous $SiO_2$ [25,26]. The IEP of Pd/AC was found to be much lower than the reported IEPs of ACs, likely due to the surface oxidation of AC in the catalyst preparation process [27,28]. As for $Pd/Al_2O_3$ with varied Pd loading

**Table 1**
Properties of $Pd/Al_2O_3$ catalysts.

| Catalyst | Pd content (wt.%) | Pd dispersion (%) | Pd particle sizes (nm) | | BET surface area ($m^2\ g^{-1}$) |
|---|---|---|---|---|---|
| | | | $d_1$ [a] | $d_2$ [b] | |
| $Pd(0.48)/Al_2O_3$ | 0.48 | 45.5 | 2.6 | 2.5 | 106.2 |
| $Pd(1.07)/Al_2O_3$ | 1.07 | 15.6 | 6.7 | 7.2 | 111.1 |
| $Pd(1.93)/Al_2O_3$ | 1.93 | 12.1 | 9.6 | 9.3 | 106.9 |
| $Pd(4.95)/Al_2O_3$ | 4.95 | 9.2 | 10.2 | 12.2 | 103.5 |

[a] Calculated from TEM.
[b] Calculated from $H_2$ chemisorption.

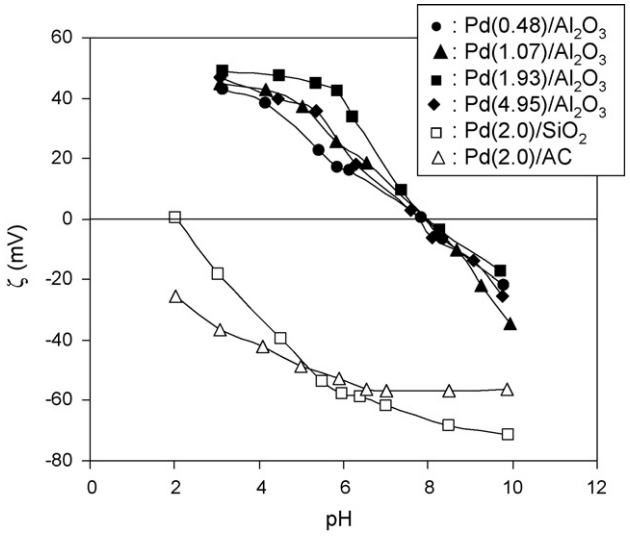


**Fig. 2.** Surface charge densities ($\zeta$) of supported catalysts as a function of solution pH.

amounts, nearly identical IEPs were observed at around 8.0, much higher than those of $Pd/SiO_2$ and Pd/AC.

TEM images of the $Pd/Al_2O_3$ catalysts with varied Pd loading amounts are compiled in Fig. 3. For $Pd(0.48)/Al_2O_3$, relatively small Pd particles with sizes of 0–5 nm were observed, whereas increasing Pd loading amount led to the formation of large Pd particles. The average particle size of Pd metal can be calculated based on a surface area weighted diameter:

$$\overline{d_s} = \frac{\sum n_i d_i^3}{\sum n_i d_i^2} \quad (1)$$

where $n_i$ is the number of counted Pd particle with diameter of $d_i$ and the total number of particles ($\sum n_i$) is larger than 100.

The average Pd particle sizes were calculated to be 2.6, 6.7, 9.6 and 10.2 nm for $Pd(0.48)/Al_2O_3$, $Pd(1.07)/Al_2O_3$, $Pd(1.93)/Al_2O_3$ and $Pd(4.95)/Al_2O_3$, respectively, indicative of the aggregation of Pd particles on the $Al_2O_3$ surface with the increase of Pd loading amount.

The Pd dispersions measured from $H_2$ chemisorption were found to be 45.5%, 15.6%, 12.1% and 9.2% for $Pd(0.48)/Al_2O_3$, $Pd(1.07)/Al_2O_3$, $Pd(1.93)/Al_2O_3$ and $Pd(4.95)/Al_2O_3$, respectively, reflecting decreased Pd dispersion, as well as enlarged Pd particle size with Pd loading amount. The corresponding average particle sizes of Pd metal in the catalysts were calculated to be 2.5, 7.2, 9.3 and 12.2 nm, which are in good agreement with the TEM observations.

TPR profiles of the calcined samples are presented in Fig. 4. The reduction behaviors differed in the samples with varied Pd loading amounts. For $Pd(0.48)/Al_2O_3$ sample, a small $H_2$ consumption peak was observed at about 78 °C. In contrast, negative $H_2$ consumption peaks were observed around 85 °C for other samples and the peak intensity increased with Pd loading amount. Seshu et al. [29] stud-

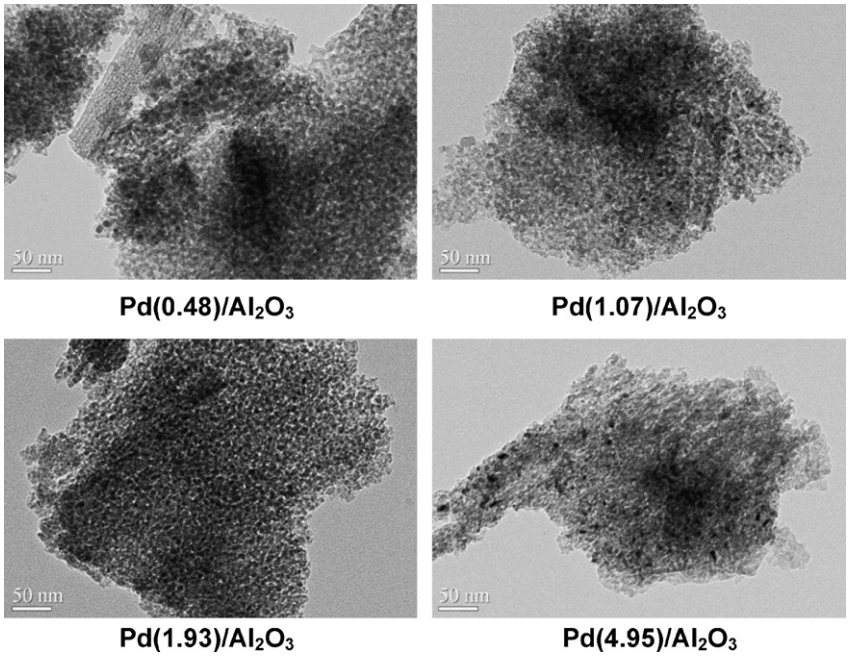


**Fig. 3.** TEM images of $Pd/Al_2O_3$ catalysts.

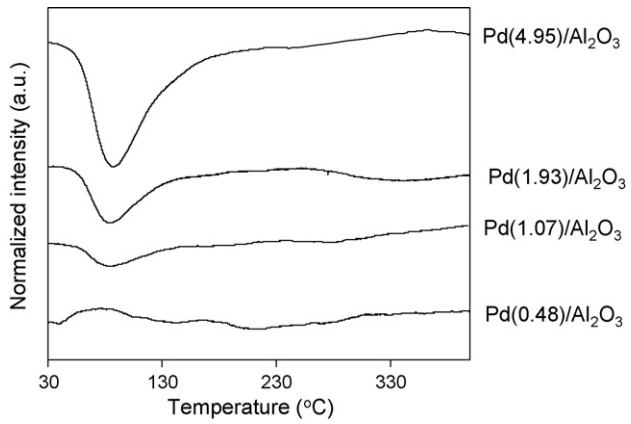


**Fig. 4.** TPR profiles of calcined $Pd/Al_2O_3$ catalysts.

ied the catalytic hydrodechloration of chlorobenzene over $Pd/Al_2O_3$ and also found that the reduction behaviors of calcined $Pd/Al_2O_3$ samples were linked with Pd loading amounts. The $H_2$ consumption peak observed for $Pd(0.48)/Al_2O_3$ could be attributed to the reduction of $PdO_xCl_y$ or PdO species with strong metal–support interaction [29–31], while the negative $H_2$ consumption peaks for calcined $Pd/Al_2O_3$ with high Pd loading amount were characteristic of the decomposition of β-PdH [23,29,32,33]. In principle, the Pd content-dependent reduction behaviors of the calcined samples are related to Pd particle size on the $Al_2O_3$ surface. Supported Pd metal with small particle size is susceptible to strong metal–support interaction due to the intrinsic size effect [34], while large Pd particles readily leads to the formation of β-PdH [23,35]. It should be emphasized that the presence of negative $H_2$ consumption peaks for the samples with high Pd loading amounts suggests that PdO species on the $Al_2O_3$ surface are susceptible to reduction by $H_2$ even below room temperature. In addition, metallic Pd on $Al_2O_3$ surface is prone to activating and storing $H_2$ at room temperature, and hence facilitates the reduction reaction under mild reaction conditions.

### 3.2. Bromate reduction over supported Pt and Pd catalysts

$SiO_2$, $Al_2O_3$ and AC are commonly used catalyst supports due to their high stability and large specific surface areas. Catalytic hydrogenation of aqueous bromate over $Pd(2.0)/SiO_2$, $Pd(1.93)/Al_2O_3$ and Pd(2.0)/AC at pH 5.6 is compiled in Fig. 5a. For $Pd(1.93)/Al_2O_3$, bromate was rapidly reduced and the residual bromate concentration after 2 h was below the detection limit (0.008 μM). It is noteworthy that the regulated maximum level for bromate in drinking water is 0.078 μM by WHO and USEPA [2,3]. During the reaction process, the sum concentrations of bromate and bromide were nearly identical to the initial bromate concentrations, indicating that bromide was the sole reduction product. Moreover, bromate reduction efficiencies varied with the catalysts tested and the removal efficiencies of bromate were 2.5%, 100% and 23.8% for $Pd/SiO_2$, $Pd/Al_2O_3$ and Pd/AC, respectively after reaction for 2 h. Thus, it is concluded that the catalytic activity is ordered as follows: $Pd/Al_2O_3 > Pd/AC > Pd/SiO_2$. In a heterogeneous catalysis process, adsorption of reactant on the catalyst surface is essential to the commencement and implementation of the catalytic reaction. Yuan and Keane [36] studied the hydrodechlorination of 2,4-dichlorophenol over $Pd/Al_2O_3$ and observed the dependency of catalytic activity and selectivity to pH, due to the pH mediated adsorptive interaction of reactions with the catalyst surface. Zeta potential measurement showed that the surface of $Pd/SiO_2$ or Pd/C was negatively charged at the test pH of 5.6, while bromate presents predominantly as an anion due to its high disassociation constant [37]. Therefore, the electrostatic repulsive interaction could markedly suppress bromate adsorption on the catalyst surface leading to a low catalytic activity of $Pd/SiO_2$ or Pd/C [36]. In contrast, the IEP of $Pd/Al_2O_3$ catalyst was around 8.0 and hence its surface is positively charged at pH 5.6, which may enhance bromate adsorption through electrostatic attractive interaction and facilitate bromate reduction.

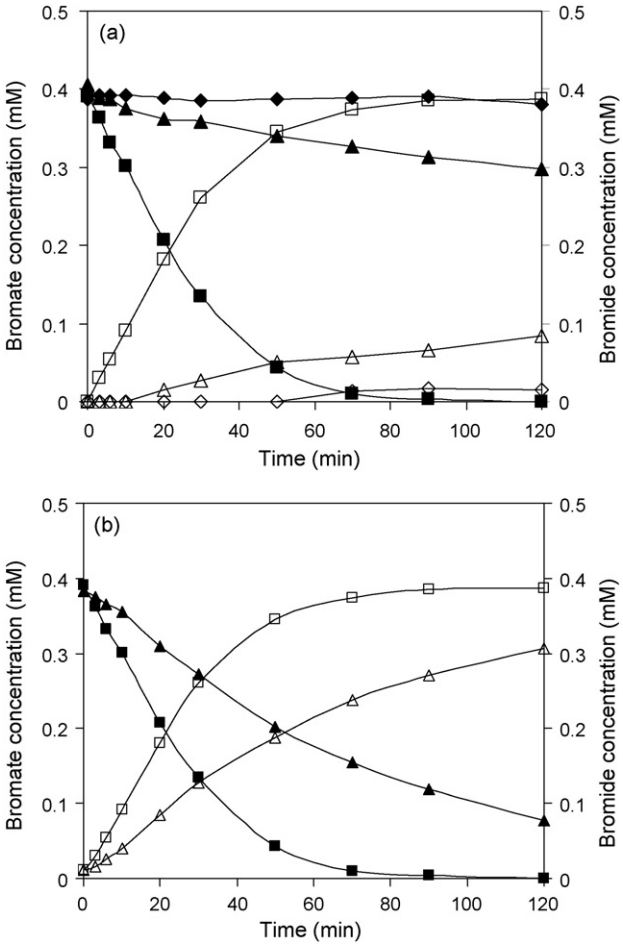


**Fig. 5.** (a) Catalytic bromate reduction over (♦, ◊) $Pd(2.0)/SiO_2$ (■, □) $Pd(1.93)/Al_2O_3$ and (▲, △) Pd(2.0)/AC catalysts and (b) catalytic bromate reduction over (■, □) $Pd(1.93)/Al_2O_3$ and (▲, △) $Pt(2.0)/Al_2O_3$ catalysts. Filled symbols denote bromate concentration and open symbols denote bromide concentration. Reaction conditions: initial bromate concentration 0.39 mM, pH 5.6.

Supported Pt and Pd catalysts are often adopted in catalytic hydrogenation due to their highly effective activation of $H_2$ at low temperature. Catalytic bromate reduction over $Al_2O_3$ supported Pt and Pd was also evaluated at pH 5.6 and the results are presented in Fig. 5b. After reaction for 30 min, approximately 30.4% of bromate was removed by $Pt/Al_2O_3$, but 65.4% by $Pd/Al_2O_3$, reflecting a higher catalytic activity of $Pd/Al_2O_3$. Because Pt and Pd metals have nearly identical adsorption heats and similar adsorption affinity toward $H_2$ [38], the higher catalytic activity of $Pd/Al_2O_3$ probably results from the higher $H_2$ adsorption capacity of Pd as compared to Pt [39]. The discussion hereafter only focuses on the bromate reduction over $Pd/Al_2O_3$ catalyst.

### 3.3. Influence of initial concentration

For heterogeneous catalysis, the catalytic reaction essentially occurs on the catalyst surface and reactant adsorption is a prerequisite step. To better understand the mechanism of catalytic bromate reduction over $Pd/Al_2O_3$, the influence of initial bromate

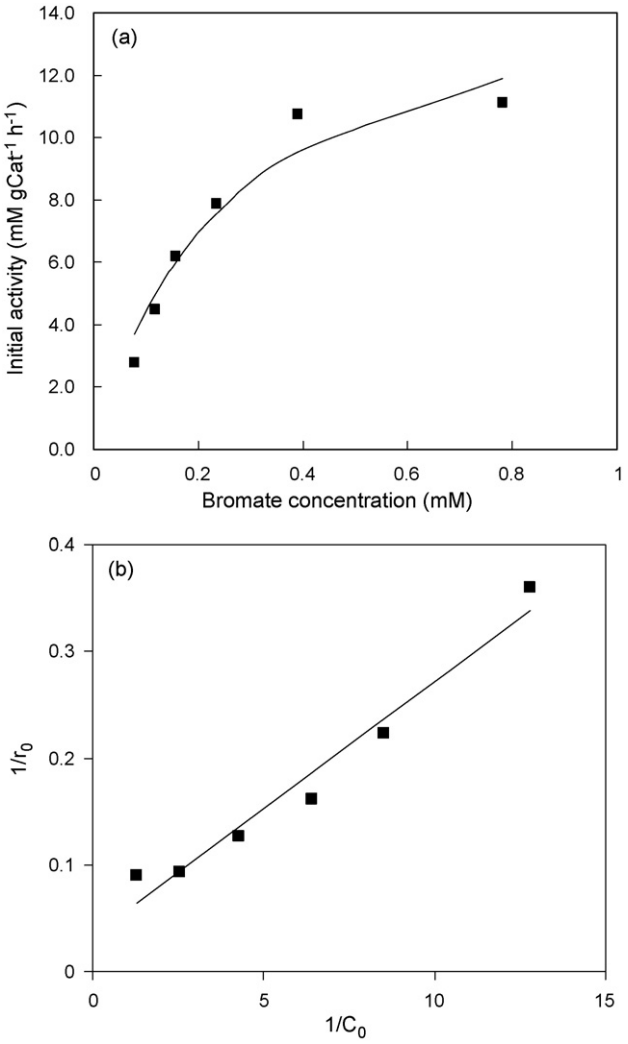


**Fig. 6.** (a) Initial bromate reduction rates as a function of initial bromate concentration and (b) linear plot of $1/r_0$ versus $1/C_0$. Reaction conditions: pH 5.6. Catalyst: Pd(1.93)/$Al_2O_3$. Catalyst dosage: 0.05 g $L^{-1}$. Line represents fitting curve using the Langmuir–Hinshelwood model.

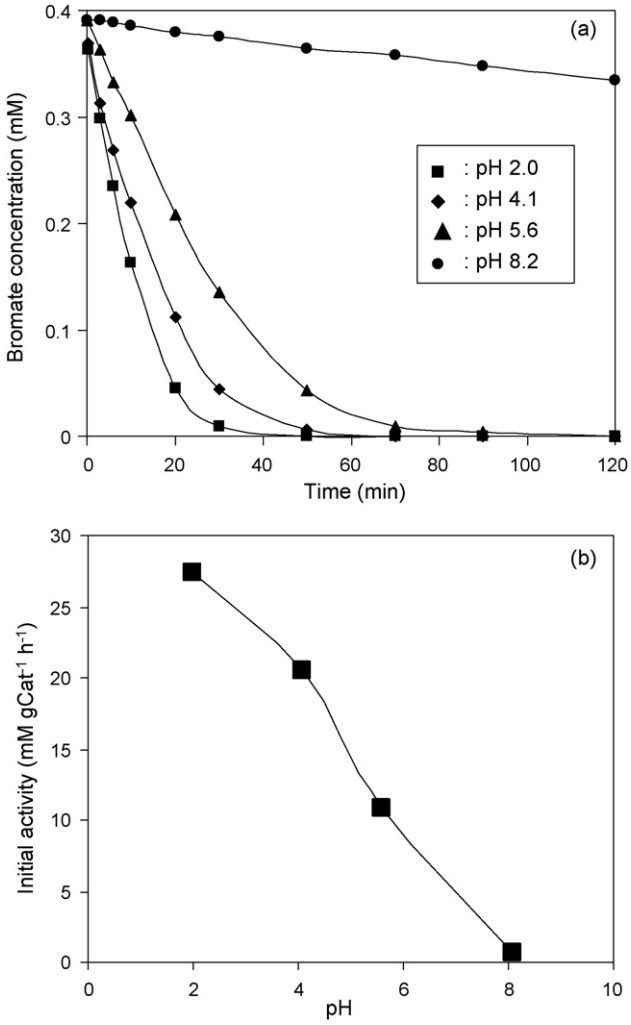


**Fig. 7.** (a) Catalytic bromate reduction over Pd(1.93)/$Al_2O_3$ at different pH and (b) dependence of initial bromate reduction rates on solution pH. Reaction conditions: initial bromate concentration 0.39 mM.

concentration on bromate reduction was evaluated. It is noteworthy that evaluation of reaction kinetics might also be affected by the mass transfer limitation. In order to test the possibility, the bromate reduction over Pd(1.93)/$Al_2O_3$ with varied catalyst dosages was compared and the results are presented in Fig. 1S (see Supporting information). Although the increase in the catalyst dosage led to enhanced bromate reduction, the initial activities remained nearly constant after catalyst mass normalization, indicative of the absence of mass transfer limitation under the tested reaction conditions [40,41].

The reduction of bromate over Pd(1.93)/$Al_2O_3$ with varied initial bromate concentrations as a function of reaction time is compared in Fig. 2S (see Supporting information) and the dependence of initial bromate reduction rate on initial bromate concentration is presented in Fig. 6. As shown in Fig. 6a, increasing initial bromate concentration from 0.08 to 0.39 mM led to the increase of the initial bromate reduction rate from 2.8 to 10.7 mM gCat$^{-1}$ h$^{-1}$, whereas with a further increase of bromate concentration the initial bromate reduction rate kept nearly constant. The above observation can be described by the Langmuir–Hinshelwood model. Assuming that $H_2$ adsorption on Pd surface is much stronger than that of bromate, the initial bromate reduction rate becomes proportional to the adsorbed bromate concentration [42]:

$$r_0 = -\frac{dC}{dt} = k\theta_s = k\frac{bC}{1+bC} \quad (2)$$

$$\frac{1}{r_0} = \frac{1}{kb}\frac{1}{C} + \frac{1}{k} \quad (3)$$

where $r_0$ is the initial bromate reduction rate at concentration $C$, $\theta_s$ is the bromate coverage on the catalyst surface, $k$ is the reaction rate constant and $b$ is the equilibrium constant for bromate adsorption on the catalyst.

The plot of $1/r_0$ versus $1/C$ is given in Fig. 6b. The good linear relationship of $1/r_0$ with $1/C$ ($R^2$ higher than 0.96) suggests that the bromate reduction by catalytic hydrogenation over supported Pd catalyst is controlled by the adsorption of bromate.

### 3.4. Influence of pH on bromate reduction

Solution pH is one of the most important parameters controlling bromate reduction in water [11,13]. The catalytic bromate reduction over Pd(1.93)/$Al_2O_3$ at varied pH is presented in Fig. 7. Increasing pH from 2.0 to 8.2 led to a decrease in the initial reduction rate of bromate from 27.3 to 0.6 mM gCat$^{-1}$ h$^{-1}$, reflecting a decreased catalytic activity of Pd(1.93)/$Al_2O_3$ with pH.

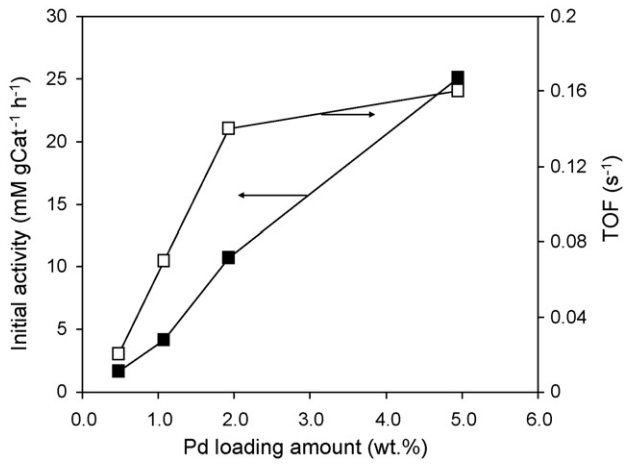


**Fig. 8.** Influence of Pd content on bromate reduction rates and TOF of the catalysts for bromate reduction. Reaction conditions: initial bromate concentration 0.39 mM, pH 5.6.

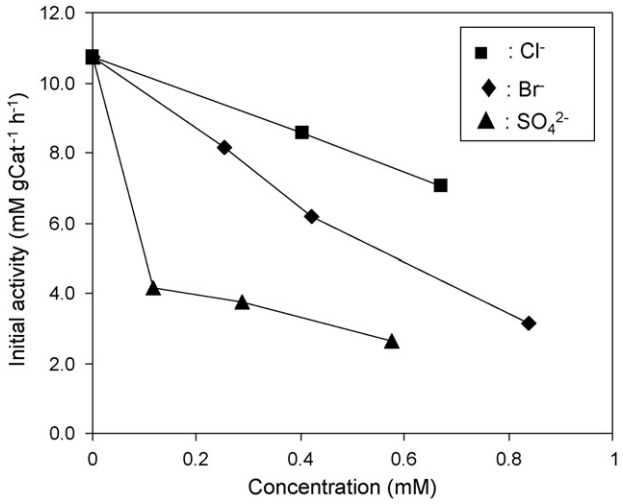


**Fig. 9.** Influence of $SO_4^{2-}$, $Cl^-$ and $Br^-$ on bromate reduction over $Pd(1.93)/Al_2O_3$. Reaction conditions: initial bromate concentration 0.39 mM, pH 5.6.

For the catalytic bromate reduction, $H_2$ was the reduction regent and the standard potential of $H_2/H^+$ was equal to zero. Hence the overall potential of the reaction was dependent on the potential of $BrO_3^-/Br^-$. Furthermore, $H_2$ adsorption on Pd surface was so strong that at room temperature the ratio of dissociated H (adsorbed on Pd surface) to surface Pd atom was almost equal to 1. In addition, $H_2$ adsorbed on Pd surface was feasible to form β-PdH (physically adsorbed) at room temperature. Consequently, the H coverage on Pd surface could be considered to be constant, because $H_2$ gas was continuously bubbled into the reaction system at a constant $H_2$ flow rate. In principle, the change in pH may impact the redox potential of the bromate anion. The bromate reduction is shown in Eq. (4) [43]:

$$BrO_3^- + 6H^+ + 6e^- \rightarrow Br^- + 3H_2O \quad (4)$$

The potential of bromate reduction to bromide can be thus calculated as follows [44]:

$$E_{BrO_3^-/Br^-} = 1.411 + \frac{0.0592}{6} \log([BrO_3^-][H^+]^6/[Br^-]) \quad (5)$$

The potential of bromate reduction to bromide is pH-dependent and increasing pH leads to a decreased potential of bromate reduction, indicative of low reducibility of bromate at high pH. Solution pH may also influence catalyst surface properties [24,36]. Zeta potentials of the catalysts decreased with pH and the IEPs of $Pd/Al_2O_3$ catalysts were about 8.0. At pH below 8.0, the catalyst surface is positively charged, which invokes an electrostatic attractive interaction between the bromate ion and the catalyst, facilitating bromate reduction by enhancing bromate adsorption. On the contrary, increasing pH attenuated the adsorptive interaction of the bromate ion lowering bromate reduction efficiency. In particular, at pH above 8.0 the catalyst surface is negatively charged, leading to an electrostatic repulsive interaction between bromate and the catalyst, and to suppressed bromate reduction [22,36].

### 3.5. Influence of Pd loading amount

Because metallic Pd provides the catalytic active site of the catalyst, increasing Pd loading amount is expected to enhance the bromate reduction via offering more reaction sites. The dependence of initial bromate reduction rate on Pd loading amount is shown in Fig. 8 and Fig. 3S (see Supporting information). Increasing Pd loading amount from 0.48 to 4.95 wt.% led to the increase in the initial reduction rate from 1.6 to 25.1 mM $gCat^{-1}$ $h^{-1}$. Deeper insight into Pd particle size dependent catalytic activity can be further gained by comparing the initial turnover frequency (TOF) of Pd site in the $Pd/Al_2O_3$ catalyst. The initial TOF is defined as the reduction rate of bromate anion per active Pd site on the $Al_2O_3$ surface within initial 10 min, where the number of active Pd sites in the catalyst was quantified using the $H_2$ chemisorption method. As shown in Fig. 8, increasing Pd loading amount from 0.48 to 1.93 wt.% led to a substantial increase of the TOF from 0.02 to 0.14 $s^{-1}$. The TOF of $Pd(4.95)/Al_2O_3$ was calculated to be 0.16 $s^{-1}$, slightly higher than that of $Pd(1.93)/Al_2O_3$. The particle size dependent Pd activity was also observed in previous studies on catalytic hydrogenation processes. For example, Aramendia et al. [45] studied catalytic hydrodechlorination of chlorobenzene in liquid phase and found that the initial TOF of the supported Pd catalyst inversely correlated to the dispersion of Pd metal, due to the effective formation of stable β-PdH on large Pd particles as compared with small Pd particles. Coq et al. [46] further pointed out that small Pd particles were partially positively charged, giving rise to low catalytic activity. Therefore, it can be concluded that for the bromate reduction metallic Pd with large particle size is more active than that with small particle size.

### 3.6. Influence of coexisting inorganic anions

The bromate reduction over $Pd/Al_2O_3$ catalyst is an adsorption controlled reaction process and follows the Langmuir–Hinshelwood model. Therefore, the presence of coexisting anions may cause competitive adsorption with bromate for the catalyst surface and consequently suppress the bromate reduction. Considering their ubiquitous presence in drinking water, $Cl^-$, $SO_4^{2-}$ and $Br^-$ (bromate reduction product) were chosen to assess the impact of coexisting anions on the bromate reduction.

Catalytic bromate reduction over $Pd(1.93)/Al_2O_3$ in the presence of $Cl^-$, $SO_4^{2-}$ and $Br^-$ with varied concentrations and the impact of anions on the catalytic activity of $Pd(1.93)/Al_2O_3$ are compared in Fig. 4S (see Supporting information) and Fig. 9, respectively. A consistent trend is observed that the presence of coexisting anions led to suppressed bromate reduction and the inhibition effect was promoted with the increase of anion concentration. In addition, the inhibition effect seemed to be related to the anion type. As shown in Fig. 9, $SO_4^{2-}$ exhibits the most prominent inhibition effect on the bromate reduction among all anions tested.

The inhibition effect of anions can be explained by the competitive adsorption of coexisting anions with the bromate ion. The

adsorption affinity to anion-exchange resins is ordered as follows: $SO_4^{2-} > Br^- > Cl^-$ [47]. The observed sequence of inhibition effects of the tested anions on the bromate reduction was consistent with the above sequence. In general, an anion with high ionic charge and small ionic size invokes strong electrostatic interaction and, therefore, is preferentially adsorbed to the positively charged catalyst surface. Compared to $Cl^-$ and $Br^-$, $SO_4^{2-}$ has higher ionic charge, resulting in stronger adsorption and thus more prominent inhibition effect on the bromate reduction. Although the bare ionic size of $Cl^-$ (0.164 nm) is smaller than that of $Br^-$ (0.180 nm), the hydrated ionic size of $Br^-$ (0.330 nm) is slightly smaller than that of $Cl^-$ (0.332 nm) [48]. Therefore, stronger inhibition effect was observed on $Br^-$ than on $Cl^-$.

## 4. Conclusions

In this study, supported noble metal catalysts were prepared and the bromate reduction by catalytic hydrogenation over the catalysts was first investigated. For bromate reduction, $Al_2O_3$ is the more appropriate catalyst support as compared to $SiO_2$ and AC due to its higher IEP. Moreover, $Pd/Al_2O_3$ exhibits higher catalytic activity than $Pt/Al_2O_3$ does. The bromate reduction over $Pd/Al_2O_3$ follows the Langmuir–Hinshelwood model, indicative of an adsorption controlled reaction mechanism. In addition, the bromate reduction is pH-dependent and the enhanced bromate reduction efficiency at low pH is attributed to the strong adsorption of bromate to the catalyst surface and the high reducibility of bromate. The bromate reduction is also related to the structural properties of Pd metal on the $Al_2O_3$ surface, wherein Pd metal with large particle size has high activity, as reflected by the high TOF for bromate reduction. The presence of coexisting anions suppresses the bromate reduction via competitive adsorption for the catalyst surface and $SO_4^{2-}$ exhibits much stronger inhibition effect than $Br^-$ and $Cl^-$ due to its higher ionic charge. Findings in this study indicate that catalytic hydrogenation is highly efficient for the removal of aqueous bromate and can be potentially used as a general treatment technique for waterborne bromate concurring with other reducible pollutants such as nitrate and chlorinated organic chemicals found in drinking water.

## Acknowledgements

The financial supports from the Natural Science Foundation of China (No. 20677026, 20877039), Scientific and Technical Supporting Programs (2006BAC02A15, 2006BAJ08B02) and Program of New Century Excellent Talents in University (NCET) are gratefully acknowledged.

## Appendix A. Supplementary data

Supplementary data associated with this article can be found, in the online version, at doi:10.1016/j.apcatb.2010.02.021.

## References

[1] W.R. Haag, J. Hoigne, Environ. Sci. Technol. 17 (1983) 261–267.
[2] H.S. Weinberg, C.A. Delcomyn, V. Unnam, Environ. Sci. Technol. 37 (2003) 3104–3110.
[3] World Health Organization, Bromate in Drinking-water. Background Document for Preparation of WHO Guidelines for Drinking-water Quality, World Health Organization Press, Geneva, 2005.
[4] W.A.M. Hijnen, R. Voogt, H.R. Veenendaal, H. Van der Jagt, D. Van der Kooij, Appl. Environ. Microbiol. 61 (1995) 239–244.
[5] C.G. van Ginkel, A.M. van Haperen, B. Van der Togt, Water Res. 39 (2005) 59–64.
[6] W.A.M. Hijnen, R. Jong, D. Van Der Kooij, Water Res. 33 (1999) 1049–1053.
[7] L. Xie, C. Shang, Chemosphere 66 (2007) 1652–1659.
[8] Q.L. Wang, S. Snyder, J. Kim, H. Choi, Environ. Sci. Technol. 43 (2009) 3292–3299.
[9] World Health Organization, Guidelines for Drinking-water Quality: Incorporating First Addendum. Vol. 1. Recommendations, 3rd ed., WHO Press, Geneva, 2006.
[10] W.J. Huang, L.Y. Chen, Environ. Technol. 25 (2004) 403–412.
[11] M. Siddiqui, W.Y. Zhai, G. Amy, C. Mysore, Water Res. 30 (1996) 1651–1660.
[12] R. Butler, A. Godley, L. Lytton, E. Cartmell, Crit. Rev. Environ. Sci. Technol. 35 (2005) 193–217.
[13] N. Kishimoto, N. Matsuda, Environ. Sci. Technol. 43 (2009) 2054–2059.
[14] K.-D. Vorlop, T. Tacke, Chem. Eng. Technol. 61 (1989) 836–837.
[15] S. Horold, K.-D. Vorlop, T. Tacke, M. Sell, Catal. Today 17 (1993) 21–30.
[16] A. Pintar, Catal. Today 77 (2003) 451–465.
[17] K.D. Hurley, J.R. Shapley, Environ. Sci. Technol. 41 (2007) 2044–2049.
[18] J.B. Hoke, G.A. Gramiccioni, E.N. Balko, Appl. Catal. B: Environ. 1 (1992) 285–296.
[19] C. Amorim, G. Yuan, P.M. Patterson, M.A. Keane, J. Catal. 234 (2005) 268–281.
[20] P.D. Vaidya, V.V. Mahajani, Appl. Catal. B: Environ. 51 (2004) 21–31.
[21] T. Kawabata, I. Atake, Y. Ohishi, T. Shishido, Y. Tian, K. Takaki, K. Takehira, Appl. Catal. B: Environ. 66 (2006) 151–160.
[22] S. Gomez-Quero, F. Cardenas-Lizana, M.A. Keane, Ind. Eng. Chem. Res. 47 (2008) 6841–6853.
[23] C. Amorim, M.A. Keane, J. Colloid Interface Sci. 322 (2008) 196–208.
[24] M.A. Ryashentseva, Russ. Chem. Rev. 64 (1995) 967–983.
[25] R.K. Iler, The Chemistry of Silica, Wiley, New York, 1979.
[26] J.M. Rosenholm, T. Czuryszkiewicz, F. Kleitz, J.B. Rosenholm, M. Linden, Langmuir 23 (2007) 4315–4323.
[27] A. Bismarck, C. Wuertz, J. Springer, Carbon 37 (1999) 1019–1027.
[28] P. Chingombe, B. Saha, R.J. Wakeman, Carbon 43 (2005) 3132–3143.
[29] B.N. Seshu, N. Lingaiah, R. Gopinath, P.S.S. Reddy, P.S. Sai Prasad, J. Phys. Chem. C 111 (2007) 6447–6453.
[30] A.B. Gaspar, L.C. Dieguez, Appl. Catal. A: Gen. 201 (2000) 241–251.
[31] C. Contescu, D. Macovei, C. Craiu, C. Teodorescu, J.A. Schwarz, Langmuir 11 (1995) 2031–2040.
[32] A. Benedetti, G. Fagherazzi, F. Pinna, G. Rampazzo, M. Selva, G. Strukul, Catal. Lett. 10 (1991) 215–224.
[33] V.H. Sandoval, C.E. Gigola, Appl. Catal. A: Gen. 148 (1996) 81–96.
[34] W.M.H. Sachtler, A.Y. Stakheev, Catal. Today 12 (1992) 283–295.
[35] B. Coq, H. Serge, F. Figueras, D. Tournigant, Appl. Catal. A: Gen. 101 (1993) 41–50.
[36] G. Yuan, M.A. Keane, Ind. Eng. Chem. Res. 46 (2007) 705–715.
[37] D.L. Kamble, S.T. Nandibewoor, Int. J. Chem. Kinet. 28 (1996) 673–679.
[38] I. Toyoshima, G.A. Somorjai, Catal. Rev. Sci. Eng. 19 (1979) 105–159.
[39] Y. Hashimoto, Y. Uemichi, A. Ayame, Appl. Catal. A: Gen. 287 (2005) 89–97.
[40] G. Yuan, M.A. Keane, Chem. Eng. Sci. 58 (2003) 257–267.
[41] O.M. Ilinitch, F. Petrus Cuperus, L.V. Nosova, E.N. Gribov, Catal. Today 56 (2000) 137–145.
[42] A. Pintar, J. Batista, J. Levec, T. Kajiuchi, Appl. Catal. B: Environ. 11 (1996) 81–98.
[43] A. Mills, G. Meadows, Water Res. 29 (1995) 2181–2185.
[44] T. Mussini, P. Longhi, in: A.J. Bard, R. Parsons, J. Jordan (Eds.), Standard Potentials in Aqueous Solution, Marcel Dekker, New York, 1985.
[45] M.A. Aramendia, V. Borau, I.M. Garcia, C. Jimenez, F. Lafont, A. Marinas, J.M. Marinas, F.J. Urbano, J. Catal. 187 (1999) 392–399.
[46] B. Coq, G. Ferrat, F. Figueras, J. Catal. 101 (1986) 434–445.
[47] W.J. Weber Jr., Physicochemical Processes for Water Quality Control, Wiley–Interscience, New York, 1972.
[48] A.G. Volkov, S. Paula, D.W. Deamer, Bioelectrochem. Bioenerg. 42 (1997) 153–160.